Structural Monitoring and Maintenance, *Vol. 11, No. 3 (2024) 203-217*
https://doi.org/10.12989/smm.2024.11.3.203

An approach for structural damage identification using electromechanical impedance

Yujun Ye[1a], Yikai Zhu[1], Bo Lei[2], Zhihai Weng[3], Hongchang Xu[2] and Huaping Wan[*1]

[1]*College of Civil Engineering and Architecture, Zhejiang University, Hangzhou 310058, China*
[2]*China Construction Third Engineering Bureau Co., Ltd., Wuhan 430064, China*
[3]*Huzhou City Investment and Development Group Co., Ltd., Huzhou 313000, China*

(*Received November 19, 2023, Revised March 10, 2024, Accepted March 13, 2024*)

Abstract. Electro-mechanical impedance (EMI) technique is a low-cost structural damage detection method. It reflects structural damage through the change in admittance signal which contains the structural mechanical impedance information. The ambient temperature greatly affects the admittance signal, which hides the changes caused by structural damage and reduces the accuracy of damage identification. This study introduces a convolutional neural network to compensate for the temperature effect. The proposed method uses a framework that consists of a feature extraction network and a decoding network, and the original admittance signal with temperature information is used as the input. The output admittance signal is eliminated from the temperature effect, improving damage identification robustness. The admittance data simulated by the finite element model of the spatial grid structure is used to verify the effectiveness of the proposed method. The results show that the proposed method has advantages in identification accuracy compared with the damage index minimization method and the principal component analysis method.

Keywords: convolutional neural network; electro-mechanical impedance; spatial grid structure structural damage identification; temperature compensation

1. Introduction

Structural damage identification methods are essential for ensuring the normal service life of civil engineering structures. Over the past decade, significant efforts have been dedicated to advancing these methods, with extensive research focused on enhancing their accuracy and robustness (Avci *et al.* 2021, Azimi *et al.* 2020; Hou and Xia 2021). Data-driven approaches, in particular, have received significant attention due to their high efficiency (Wan and Ni 2018, Wan and Ni 2019, Wan *et al.* 2024).

Electro-mechanical impedance (EMI) technology is a low-cost method for detecting structural damage. It utilizes the direct and converse piezoelectric effects of piezoelectric materials to obtain admittance signals when bonded to the host structure. The signals of admittance contain information about the structural mechanical impedance, which can be utilized to detect structural

*Corresponding author, Ph.D., E-mail: hpwan@zju.edu.cn
[a]Ph.D. Student

http://www.techno-press.org/?journal=smm&subpage=7 ISSN: 2288-6605 (Print), 2288-6613 (Online)

damage. EMI technology is sensitive to early structural damage and has been successfully used to identify structural irregularities such as bolt loosening (Qiu and Li 2022), steel corrosion (Morwal *et al*. 2023), and concrete damage (Zhao *et al*. 2023). This demonstrates its wide range of potential applications (Park *et al*. 2003, Na and Baek 2018). A significant amount of research has focused on enhancing the efficiency and precision of EMI-based damage detection. Parida *et al*. (2022) integrated deep learning techniques with EMI technology and utilized a pre-trained Convolutional Neural Network-Long Short-Term Memory hybrid model to accurately predict the health status signals of reinforced concrete structures, thus enabling the evaluation of structural damage. Lu *et al.* (2023) developed a nonlinear EMI method and proposed the baseline-free damage index for detecting and quantifying fatigue cracks in aluminum beams.

Changes in environmental temperature can impact the EMI admittance signal, as temperature fluctuations alter the characteristics of the piezoelectric transducer. These alterations can introduce deviations to the measured signal, potentially influencing the identification of structural damage. To address this issue, compensating for the temperature effect is necessary. Park *et al.* (1999) conducted horizontal and vertical offsets on unknown operating condition signals to minimize their root mean square deviation (RMSD) from the reference signal for temperature compensation. Koo *et al.* (2009) then proposed an effective frequency shift method based on this approach, which involves finding the frequency shift that maximizes the correlation between two sets of signals. Baral *et al.* (2023) utilized regression algorithms to examine pre-collected admittance signals. They developed temperature compensation equations for admittance signals in both horizontal and vertical dimensions for unknown state signals. This method effectively mitigates the impact of temperature when the chosen frequency range is appropriate. However, the frequency shift of the signal caused by temperature is generally nonlinear, and its amplitude generally increases with the increase of frequency. This makes the above methods sensitive to the selection of frequency range, which increases the difficulty of modelling temperature compensation methods. If the selected frequency range is too broad or if the peaks in the frequency range are unsuitable, it could lead to a decrease in the accuracy of damage detection.

With the development of deep learning technology, the Convolutional Neural Network (CNN) has been used to eliminate temperature effects in admittance signals and address the aforementioned limitations. Rezende *et al.* (2020) developed a 5-layer 1D CNN network to classify the integrity states of beams at various temperatures. Du *et al.* (2021) introduced a multitask CNN capable of compensating for temperature and classifying damage, effectively distinguishing bolt loosening damage types across a wide temperature range. Li *et al.* (2021) established an electromechanical admittance database by an Orthogonal Matching Pursuit algorithm, and a CNN trained on this database achieved structural damage quantification at different temperatures. These methods utilize admittance signals under structural damage conditions as training data for network models, which are often challenging to obtain in practical scenarios. To address this limitation, this article proposes a modified CNN-based approach, which only necessitates the dataset collected in the non-destructive state of the structure. The pre-trained model can mitigate the temperature effect of the admittance signal under non-destructive states, and the proposed method enhances the robustness of structural damage identification.

2. Structural damage identification based on EMI

2.1 Mechanical impedance of structure

Assuming a resonant force $F(t)$ with a frequency f acts on a point of the structure, the resonant force $F(t)$ can be represented by the projection of a rotating phasor F in a complex plane on the real axis. At any instant of time t, the rotating phasor F can be expressed in complex form as

$$F = F_0 \cos \omega t + jF_0 \sin \omega t = F_0 e^{j\omega t} \tag{1}$$

where F_0 is the magnitude of the phasor F; $j = \sqrt{-1}$; ω is angular frequency.

The $F(t)$ causes a displacement response $u(t)$ at the point of application, and its derivative represents the velocity response $\dot{u}(t)$, which can also be represented by the projection of the rotating vector $\dot{u}$ on the real axis. $\dot{u}$ has the same rotational angular frequency with F, but it lags behind F a phase φ due to the mechanical impedance of the structure. The velocity rotation phasor $\dot{u}$ can be expressed in complex form as

$$\dot{u} = \dot{u}_0 \cos(\omega t - \varphi) + j\dot{u}_0 \sin(\omega t - \varphi) = \dot{u}_0 e^{j(\omega t - \varphi)} \tag{2}$$

where $\dot{u}_0$ is the magnitude of the velocity and φ is the phase angle between $\dot{u}$ and F.

The mechanical impedance Z at the point of application is defined as the ratio of the resonant force phasor F to the velocity phasor $\dot{u}$, and it can be expressed as

$$Z = \frac{F}{\dot{u}_0} = \frac{F_0 e^{j\omega t}}{\dot{u}_0 e^{j(\omega t - \varphi)}} = \frac{F_0}{\dot{u}_0} e^{j\varphi} \tag{3}$$

The mechanical impedance Z of the structure is a constant value at a specific frequency, and it is affected by the stiffness and damping of the structure. When the structure is damaged, its stiffness and damping properties change significantly, causing alterations in its mechanical impedance. Therefore, changes in mechanical impedance can accurately indicate structural damage and can be used to detect it.

2.2 Structural damage identification

The EMI technology primarily relies on piezoelectric ceramics (PZT) to obtain admittance signal by their coupled electromechanical properties. When the PZT patch is mechanically strained, it produces an electric voltage, called the direct piezoelectric effect. Conversely, when an electric field is applied across the PZT, it causes mechanical strains, called the converse piezoelectric effect. Because of this characteristic, a PZT patch can function as both a sensor and an actuator simultaneously.

In EMI technology, a PZT patch is generally bonded to the surface of the host structure. When detecting, the measuring device applies a sinusoidal voltage V to the patch through a wire as an excitation signal. Due to the converse piezoelectric effect, PZT undergoes periodic expansion and contraction. However, its deformation is limited due to the coupling effect between the patch and the host structure. The deformation can be indirectly measured by the charges moving to the upper and lower plane due to the direct piezoelectric effect. The charge forms a current I through the wire and returns to the measuring device, which is recorded in the form of admittance. The admittance signal of the PZT-structure coupling system can be obtained by setting excitation signals of different frequencies within the frequency range to be measured.

In the two-dimensional electromechanical coupling model, it is commonly assumed that the mechanical and piezoelectric properties of PZT are isotropic in the x-y plane. The ideal admittance is a complex function that varies with angular frequency (Bhalla and Soh 2004), expressed as

$$\begin{aligned}\overline{Y} &= G + jB \\ &= \omega j \frac{wl}{h}\left[\left(\bar{\varepsilon}_{33}^{T} - d_{31}^{2}\overline{Y}_{11}^{E}\right)\right. \\ &\quad \left.+\left(\frac{Z_a}{Z_s + Z_a}\right) d_{31}^{2}\overline{Y}_{11}^{E}\left(\frac{\tan \kappa l}{\kappa l}\right)\right]\end{aligned} \tag{4}$$

where G represents the conductance (real part of admittance) and B represents the susceptance (imaginary part of admittance); l, w, h are the length, width and thickness of PZT patch, respectively; $\bar{\varepsilon}_{33}^{T}$ is the complex dielectric permittivity; d_{31} is the strain coefficients; $\overline{Y}_{11}^{E}$ is complex Young's modulus; Z_a and Z_s are the mechanical impendances of PZT and host structure, respectively; κ is 2D wave number.

Structure damage would result in frequency shifts of the admittance signal, and the conductance is generally more sensitive. Set the non-destructive structural state at a specific temperature as the reference condition, and the conductance signal under the reference condition is considered the reference conductance. The Root Mean Square Deviation (RMSD) is used as the index to measure the difference between the conductance being evaluated and the reference conductance. It is sensitive to both the frequency shift and amplitude changes, which can be expressed as

$$\mathrm{RMSD} = \sqrt{\frac{\sum_{i=1}^{N}\left[G^{*}\left(\omega_i\right) - G\left(\omega_i\right)\right]^2}{\sum_{i=1}^{N}\left[G\left(\omega_i\right)\right]^2}} \tag{5}$$

where $G^{*}\left(\omega_i\right)$ is the conductance to be evaluated at the i$^{\mathrm{th}}$ frequency; $G\left(\omega_i\right)$ is the reference conductance. To detect the state of structural damage, an Upper Control Limit (UCL) is established by RMSD indexes of conductance dataset collected in the non-destructive structural state, expressed as

$$\mathrm{UCL} = \mu + 3\sigma \tag{6}$$

where μ and σ are the average and standard deviation of the RMSD index, respectively. When the RMSD index exceeds the UCL, the host structure is considered abnormal. However, the RMSD index cannot differentiate between the effects of environmental temperature and structural damage on conductance signals. Therefore, temperature changes would result in reduced accuracy of damage detection and temperature compensation is needed for signals to eliminate the influence of temperature on structural damage identification.

3. Temperature compensation method based on CNN

A typical CNN consists of multiple feature layers, which can be categorized into convolutional and pooling layers based on their functions. Convolutional layers are the main component of a

CNN and are used to extract the signal features. The convolutional layer contains several convolution kernels, each consisting of a parameter matrix of the same shape. The convolutional layer takes the output of the previous feature layer as input and produces a set of data by convolving the kernels with input features at a specific step size. 1D convolution can be expressed as

$$y_j^l = f\left(\sum_{i\in M_j} x_i^{l-1} w_{ij}^l + b_i^l\right) \tag{7}$$

where y_j^l is the output of the j^{th} neuron in the l^{th} layer; x_i^{l-1} is the output of the i^{th} neuron in the $(l\text{-}1)^{th}$ layer; $f(\bullet)$ is the activation function; w_{ij}^l is the kernel from the i^{th} neuron in the $(l\text{-}1)^{th}$ layer to the j^{th} neuron in the l^{th} layer; b_j^l is the bias of the j^{th} neuron in the l^{th} layer; M_j is the set of input feature maps.

Generally, the convolutional layer is followed by a pooling layer, which is used to compress data and prevent overfitting of the network due to excessive data volume. The principle is to replace the feature values in a specific region with the most representative one, usually the maximum value. The pooling function for the max pooling layer can be expressed as

$$\left(y_j^l\right)_{\max-\text{pooling}} = \max\left(x_i^{l-1}\right) \tag{8}$$

The training process of CNN is to adjust network parameters to minimize the difference between the output and the target, which is defined as the loss function. In each epoch of model training, an optimization algorithm calculates the gradient of the loss function and backpropagates to update the model weights and biases. This article utilizes the Adam optimization algorithm for network training (Kingma and Ba 2015). The model's output is the conductance after temperature compensation, and the target value is the reference conductance. The defined loss function consists of two parts. The first part aims to ensure that the compensated conductance closely matches the reference conductance. Therefore, the Mean Square Error (MSE) loss function is used to measure the difference between the two conductances, which can be expressed as

$$\mathrm{L}_{\mathrm{MSE}} = \mathrm{E}\left[\left(\hat{G}(\omega) - G(\omega)\right)^2\right] \tag{9}$$

where $\hat{G}(\omega)$ is the compensated conductance and $\mathrm{E}[\bullet]$ is the calculation of the mean value.

The second part aims to address the non-smooth characteristics of the output by introducing a Total Variation (TV) regularizer to reflect its smooth characteristics, which is represented as

$$\mathrm{L}_{\mathrm{TV}} = \mathrm{E}\left[\left(\frac{\partial\sigma(\omega)}{\partial\omega}\right)^2\right] \tag{10}$$

where $\sigma(\omega) = \hat{G}(\omega) - G(\omega)$. Therefore, the loss function of CNN can be expressed as

$$\begin{aligned}\mathrm{L} &= \mathrm{L}_{\mathrm{MSE}} + \lambda_{\mathrm{TV}}\mathrm{L}_{\mathrm{TV}} \\ &= \mathrm{E}\left[\left(\hat{G}(\omega) - G(\omega)\right)^2\right] + \lambda_{\mathrm{TV}}\mathrm{E}\left[\left(\frac{\partial\sigma(\omega)}{\partial\omega}\right)^2\right]\end{aligned} \tag{11}$$

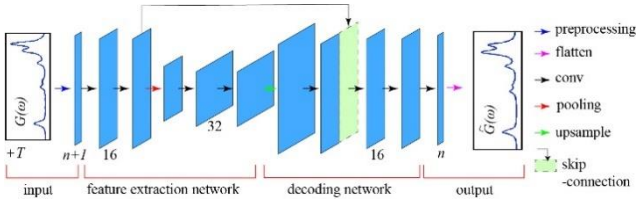

Fig. 1 Network architecture with skip-connection function

where λ_{TV} represents the tradeoff parameter of the TV regularizer, it is recommended to take a value of 0.02 (Sushmita *et al*. 2023).

The temperature compensation network utilizes a 1D CNN with a skip-connection function, and its architecture is shown in Fig. 1. The specific steps are as follows:

(1) The input consists of conductance signal and temperature information. The conductance signal is evenly divided into n frequency bands and combined with temperature information to form an n+1 channel one-dimensional signal.

(2) The feature extraction network consists of two convolutional blocks, each composed of two convolutional layers. The convolutional blocks are downsampled through a max pooling layer. The number of feature signal channels through the network doubles and the length halves.

(3) Within the decoding network, the input is first upsampled using linear interpolation. Then, the feature signal is convolved and connected to the corresponding feature layer in the feature extraction network by the channel. Finally, the feature signal passes through a convolutional block. The output length of this network is restored.

(4) The output is the compensated conductance signal. It maps the number of channels for decoding network output features to n through a convolutional block and concatenates them based on the frequency band.

4. Numerical simulation

4.1 Modeling of spatial grid structure

To demonstrate the effectiveness of the proposed method, a spatial grid structure model was carried out for electromechanical coupling simulation. The model dimensions can be found in Fig. 2. The members are all solid round rods with a diameter of 10 mm, and the nodes of the members are connected by bolt-balls with a diameter of 30 mm. Both the bolt-ball and rod are made of aluminum, with a density of 2780 kg/m^3, an elastic modulus of 72.4 GPa, and a Poisson's ratio of 0.33. A PZT patch, sized mm, is used to detect the admittance signal, made of APC-850, and the bolt-ball has a PZT patch bonded using an epoxy adhesive. The APC-850 density is 7600 kg/m^3, and the elastic modulus is 97 GPa. The adhesive density is 1180 kg/m^3, and the elastic modulus is 2 GPa.

In finite element analysis, ABAQUS was used to model the spatial grid structure and simulate its interaction with the PZT patch. Fig. 3 displays the finite element model, which includes bolt-balls, members, a PZT patch, and an adhesive layer. The bolt-ball is modeled using C3D10 elements, the rod is modeled using B31 elements, the PZT patch is modeled using C3D20RE

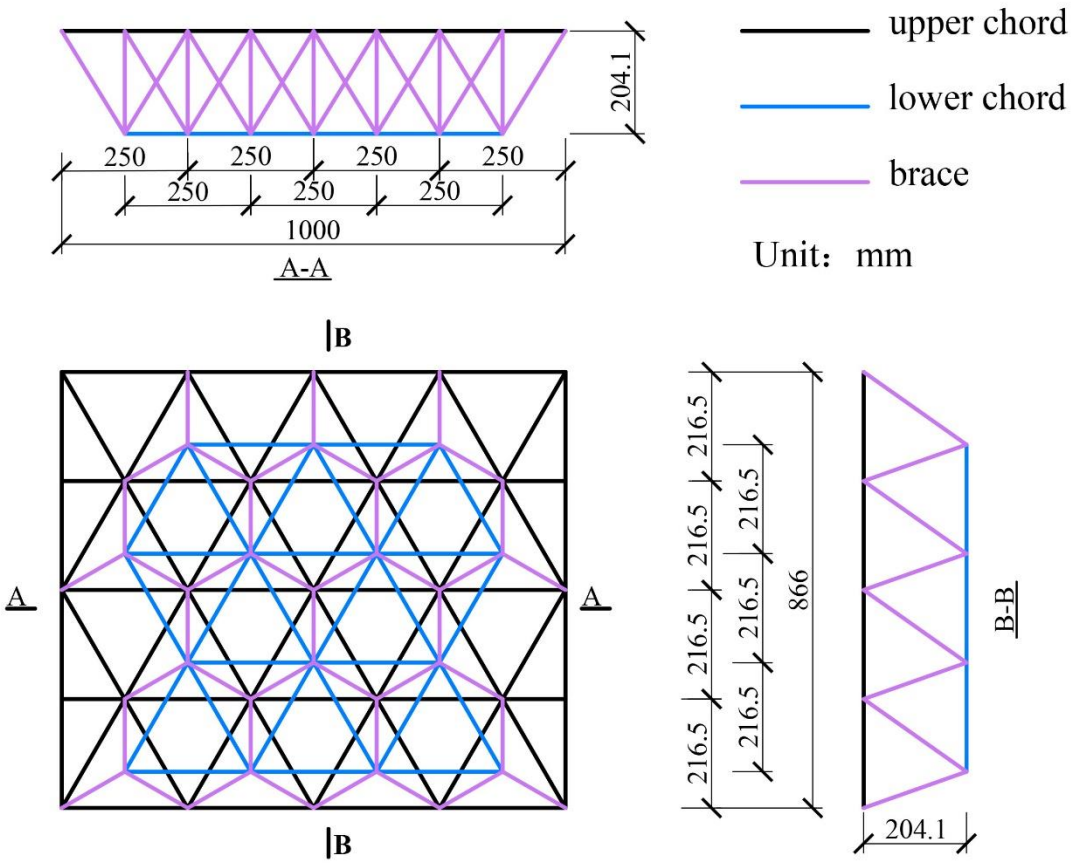

Fig. 2 Dimension size of the spatial grid structure model

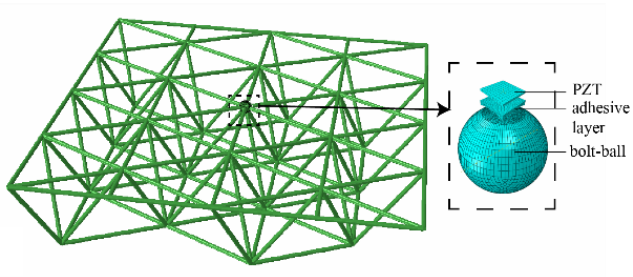

Fig. 3 Finite element model

elements, and the adhesive layer is modeled using C3D10 elements. Each component is partitioned using a grid, with the size and shape illustrated in Fig. 3. The upper surface of the adhesive layer is bonded to the PZT patch by the tie type, as is the lower surface of the adhesive layer bonded to the bolt ball. The selected frequency range is 140 kHz to 190kHz. During the harmonic analysis, a 1V

AC voltage was applied to the top surface of the piezoelectric element and the side connected to the bolt-ball was grounded. After the simulation is completed, take the total charge $Q(\omega)$ on the surface of the PZT patch at each frequency, and the current signal could be derived through its derivation of time $I(\omega)=j\omega Q(\omega)$ and admittance signal could be represented as $Y(\omega)=I(\omega)/V(\omega)$.

4.2 Damage identification

There are 9 different temperature testing conditions: -20℃, -10℃, 0℃, 10℃, 20℃, 30℃, 40℃, 50℃, and 60℃. Each testing condition includes non-destructive structural conditions and four structural damage conditions simulated by missing different numbers of members, as shown in Fig. 4, where the red color represents missing members.

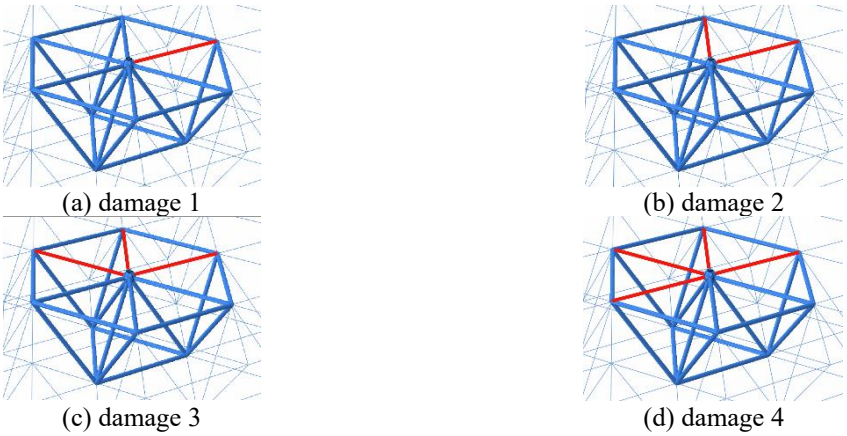

Fig. 4 Four types of structural damage conditions

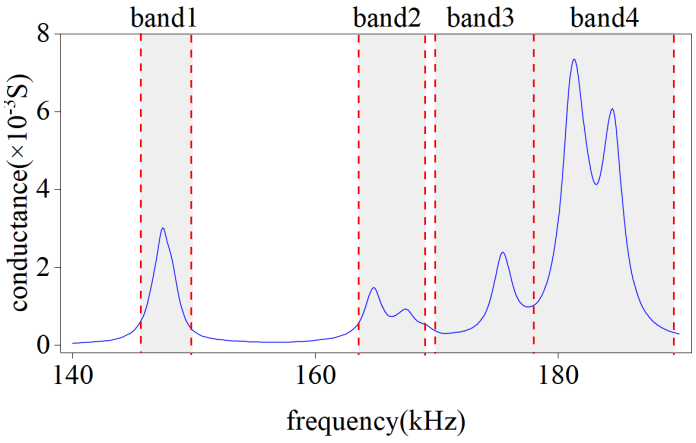

Fig. 5 Baseline conductance signal

The calculation results consist of 45 sets of admittance signals, each with a length of 500. The conductance signal in non-destructive structural conditions at 20 ℃ is selected as the reference signal. The reference signal is shown in Fig. 5, and it exhibits 6 peaks in the calculation frequency region. Based on the characteristics of the reference signal, 4 frequency bands from the calculation frequency region are selected, namely 146 kHz-150 kHz, 164 kHz-169 kHz, 170 kHz-178 kHz, and 178 kHz-190 kHz.

Fig. 6 displays the conductance signals at various temperatures under non-destructive structural conditions. As the temperature rises, the signal peaks shift to the left, with a greater degree of shift at higher frequencies. Additionally, all peak values increase, except for the right peak in band 4. Fig. 7 illustrates the conductance signals at 20°C under different structural conditions, showing that the response pattern of each peak varies depending on its frequency. The signal peak in band 1 shifts to the left as the degree of damage increases, while the signal peak position in band 3 remains almost unchanged. Moreover, the double peaks in both band 2 and band 4 exhibit significant changes in frequency and amplitude as the degree of damage increases.

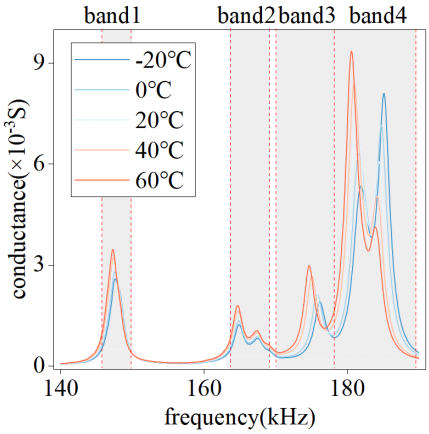

Fig. 6 Conductance signals at different temperatures under undamaged conditions

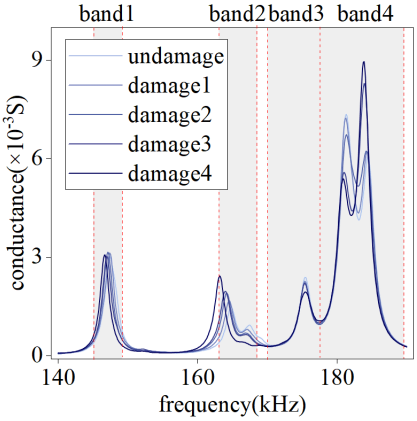

Fig. 7 Conductance signal at 20°C under different structural conditions

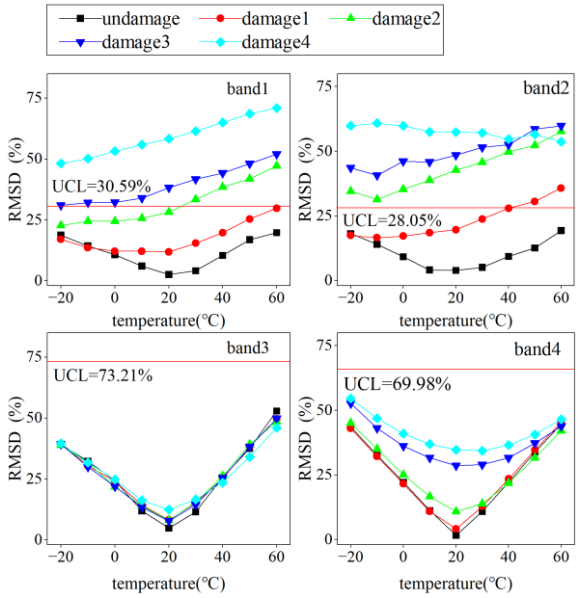

Fig. 8 RMSD index of original conductance signal

Fig. 8 displays the RMSD index of the original conductance signals across all operating conditions. When severe damage occurs to the structure, the RMSD index of the conductance signal exceeds the UCL in band 1 and band 2, but it is completely hidden in band 3 and band 4. These results suggest that the sensitivity of conductance signals to temperature changes and structural damage varies across different frequency bands. Additionally, changes in environmental temperature are likely to conceal signal changes caused by structural damage. Therefore, it is difficult to distinguish the differences between the two only using the RMSD index.

4.3 Results of temperature compensation

The conductance signals of the non-destructive state in five temperatures (-20℃, 0℃, 20℃, 40℃, and 60℃) were used to construct the training dataset. The signals, each with a length of 500, were divided into 5 frequency bands and combined with the temperature signals by channel. To each group, 100 sets of random noise with a signal-to-noise ratio of 25 were added, resulting in 500 sets of 6-channel one-dimensional signals, each with a length of 100, for model training.

The training network framework and loss function are as introduced in Section 3. The convolutional kernel size in the convolutional block is 3, while the remaining convolutional layers utilise a kernel size of 2. The stride of the pooling layer is 2. The training set and validation set were divided in a 4:1 ratio during the training process. The upper limit of training epochs set at 500 with a batch size of 6 and a learning rate of 0.0001. The network was established and trained using the PyTorch platform.

Once the training was completed, the conductance signals under 45 working conditions were used as the input of the network for testing the temperature compensation effect.The outputs of the temperature compensation network are compared with the conductance grouped by temperature, as shown in Fig. 9. It is evident that the compensated conductance signals of the undamaged state at

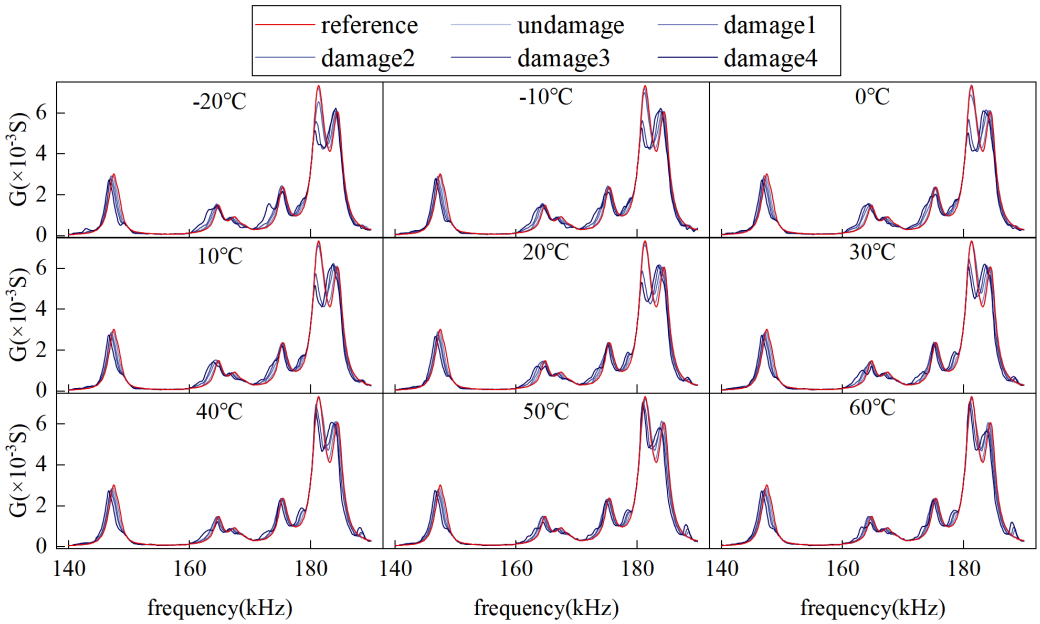

Fig. 9 Temperature compensation results under different conditions

different temperatures closely match the reference conductance. This indicates that the proposed method effectively compensates for the impact of temperature changes on the conductance signal under undamaged conditions. For the compensated signals under various damage conditions, there is a deviation from the reference signal at all temperatures, and its degree increases with the severity of structural damage. It indicates that the proposed method retains the changes in conductance signals caused by structural damage.

To further verify the effectiveness of damage detection, the RMSD index and UCL of the compensated conductance signals were calculated in each frequency band, as shown in Fig. 10. The RMSD indices under structural damage states are all above UCL, indicating that the existence of structural damage can be accurately reflected. After temperature compensation, the damage indices under the same structural state are clearly distinguished according to different temperatures, thus enabling the detection of the severity of damage.

4.4 Method comparison

The damage index minimization method is a temperature compensation method, and its principle is to minimize the difference between the unknown signal and the reference signal through frequency shift and amplitude scaling. In this study, the method was implemented using a differential algorithm to compensate for temperature effects in conductance signals. The RMSD index of the compensated signals in four frequency bands was then calculated. The results, as shown in Fig. 11, indicate that the effectiveness of the method depends on the choice of frequency bands. The RMSD index in band 1 and band 2 clearly distinguished between the undamaged and damaged states of the structure when compared to the UCL. However, the compensation effect is not ideal in band 3 and band 4, as the compensated conductance signal failed to identify the

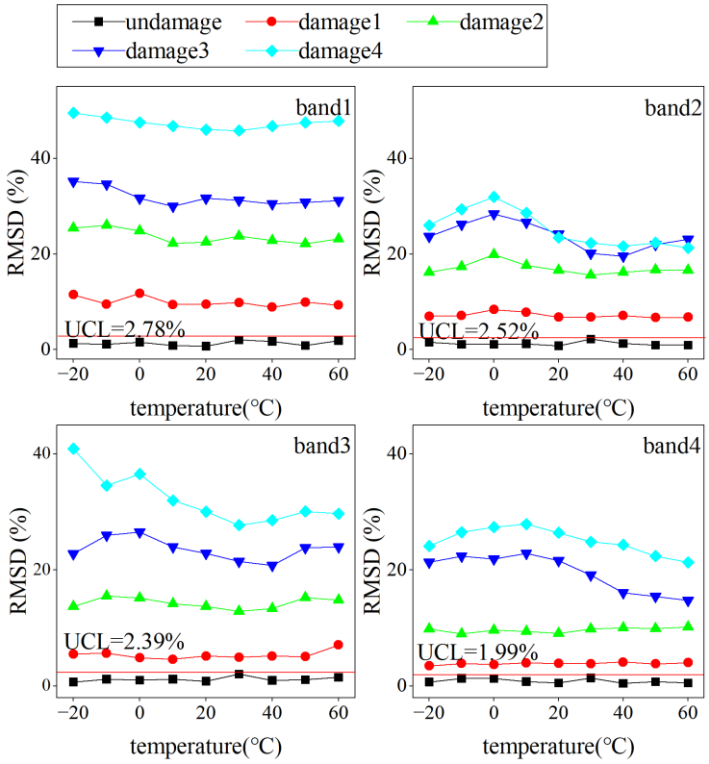

Fig. 10 RMSD index after compensation using CNN method

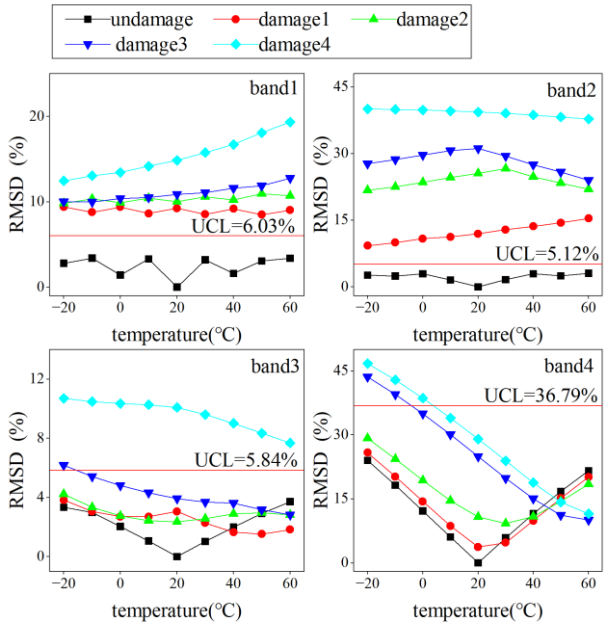

Fig. 11 RMSD index after compensation using the index minimization method

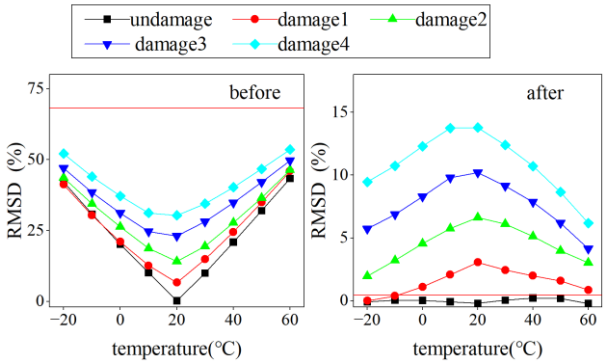

Fig. 12 RMSD index before and after using the PCA method

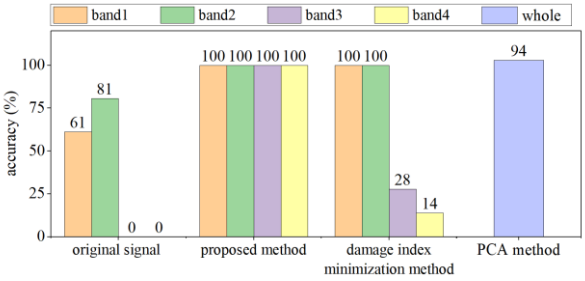

Fig. 13 Comparison of damage detection accuracy

damaged state of the structure. The damage index of the original conductance signal indicates that the conductivity signals in band 1 and band 2 are more sensitive to structural damage, while the conductance signals in band 3 and band 4 are more sensitive to temperature changes. Therefore, the temperature compensation effect of this method is more effective in the former frequency bands.

The Principal Component Analysis (PCA) method can filter out abnormal damage indices caused by temperature (Huynh *et al.* 2018). The principle of it is to compress the original signal into n dimensions by n damage indices in different frequency bands, and extract the principal component axes of the n-dimensional signals at different temperatures in the non-destructive state. When there is a signal under unknown conditions to be determined, compress it to n-dimensional in the same way, and then filter it by zeroing its projection on the principal component axis. The average value of the filtered signal is used as the final damage index. Set RMSD as the damage index and calculate the final damage index under various operating conditions before and after using the PCA method, the result is shown in Fig. 12. The results indicate that the PCA method is capable of distinguishing the final damage indices of conductance signals in undamaged and damaged structural state near the temperature of the reference condition. However, the method may fail in cases of excessive temperature changes. In such instances, the signal change caused by temperature variation could overshadow the impact of structural damage, leading to missed reporting of structural damage.

Compare the accuracy of damage detection between the original signals and the signal

processed by the three methods mentioned above, and the results are shown in Fig. 13. It is evident that the proposed method achieves 100% accuracy in damage detection for each frequency band, surpassing the accuracy obtained from the original signal. In comparison to the damage index minimization and the PCA method, the proposed method does not necessitate frequency band selection and is applicable across a wide range of temperatures

5. Conclusions

This study proposed a method based on a modified convolutional neural network to address the impact of temperature on conductance signals and enhance the accuracy of identifying structural damage. The effectiveness of the method is confirmed through finite element model analysis of the spatial grid structure. The conclusions are as follows: (1) The proposed method successfully compensates for the impact of temperature variation on the conductance signal in the undamaged structural state while retaining the changes due to structural damage. The compensated conductance signal can reflect the structural damage status through the RMSD index and UCL; (2) In comparison to the damage index minimization method and the PCA method, the proposed method demonstrates higher accuracy in damage identification across various frequency bands and wide temperature ranges.

References

Avci, O., Abdeljaber, O., Kiranyaz, S., Hussein, M., Gabbouj, M. and Inman, D.J. (2021), "A review of vibration-based damage detection in civil structures: From traditional methods to Machine Learning and Deep Learning applications", *Mech. Syst. Signal Pr.*, **147**, 107077. https://doi.org/10.1016/j.ymssp.2020.107077.

Azimi, M., Eslamlou, A.D. and Pekcan, G. (2020), "Data-driven structural health monitoring and damage detection through deep learning: State-of-the-art review", *Sensors*, **20**(10), 2778. https://doi.org/10.3390/s20102778.

Baral, S., Negi, P., Adhikari, S. and Bhalla, S. (2023), "Temperature compensation for reusable piezo configuration for condition monitoring of metallic structures: EMI approach", *Sensors*, **23**(3), 1587. https://doi.org/10.3390/s23031587.

Bhalla, S. and Soh, C.K. (2004), "Structural health monitoring by piezo-impedance transducers. I: modeling", *J. Aerosp. Eng.*, **17**(4), 154-165. https://doi.org/10.1061/(ASCE)0893-1321(2004)17:4(154).

de Rezende, S.W.F., de Moura, J.D.R.V., Neto, R.M.F., Gallo, C.A. and Steffen, V. (2020), "Convolutional neural network and impedance-based SHM applied to damage detection", *Eng. Res. Express*, **2**(3), 035031. https://doi.org/10.1088/2631-8695/abb568.

Du, F., Wu, S., Xu, C., Yang, Z. and Su, Z. (2021), "Electromechanical impedance temperature compensation and bolt loosening monitoring based on modified Unet and multitask learning", *IEEE Sensors J.*, **23**(5), 4556-4567. https://doi.org/10.1109/JSEN.2021.3132943.

Hou, R. and Xia, Y. (2021), "Review on the new development of vibration-based damage identification for civil engineering structures: 2010–2019", *J. Sound Vib.*, **491**, 115741. https://doi.org/10.1016/j.jsv.2020.115741.

Huynh, T.C., Dang, N.L. and Kim, J.T. (2018), "PCA-based filtering of temperature effect on impedance monitoring in prestressed tendon anchorage", *Smart Struct. Syst.*, **22**(1), 57-70. https://doi.org/10.12989/sss.2018.22.1.057.

Kingma, D.P. and Ba, J. (2014), "Adam: A method for stochastic optimization", *arXiv preprint*

*arXiv:*1412.6980.

Koo, K.Y., Park, S., Lee, J.J. and Yun, C.B. (2009), "Automated iImpedance-based structural health monitoring incorporating effective frequency shift for compensating temperature effects", *J. Intell. Mater. Syst. Struct.*, **20**(4), 367-377. https://doi.org/10.1177/1045389X08088664.

Li, H., Ai, D., Zhu, H. and Luo, H. (2021), "Integrated electromechanical impedance technique with convolutional neural network for concrete structural damage quantification under varied temperatures", *Mech. Syst. Signal Pr.*, **152**, 107467. https://doi.org/10.1016/j.ymssp.2020.107467.

Lu, R., Shen, Y., Zhang, B. and Xu, W. (2023), "Nonlinear Electro-Mechanical Impedance Spectroscopy for fatigue crack monitoring", *Mech. Syst. Signal Pr.*, **184**, 109749. https://doi.org/10.1016/j.ymssp.2022.109749.

Morwal, T., Bansal, T., Azam, A. and Talakokula, V. (2023), "Monitoring chloride-induced corrosion in metallic and reinforced/prestressed concrete structures using piezo sensors-based electro-mechanical impedance technique: A review", *Measurement*, **218**, 113102.7. https://doi.org/10.1016/j.measurement.2023.113102.

Na, W.S. and Baek, J. (2018), "A review of the piezoelectric electromechanical impedance based structural health monitoring technique for engineering structures", *Sensors*, **18**(5), 1307. https://doi.org/10.3390/s18051307.

Parida L., Moharana, S., Ferreira, V.M., Giri, S.K. and Ascensão, G. (2022), "A novel CNN-LSTM hybrid model for prediction of electro-mechanical impedance signal based bond strength monitoring", *Sensors*, **22**(24), 9920. https://doi.org/10.3390/s22249920.

Park, G., Sohn, H. and Farrar, C.R. (2003), "Overview of piezoelectric impedance-based health monitoring and path forward", *Shock Vib. Digest*, **35**(6), 451-464.

Park, G., Kabeya, K., Cudney, H.H. and Inman, D.J. (1999), "Impedance-based structural health monitoring for temperature varying applications", *JSME Int. J.*, **42**(2), 249-258. https://doi.org/10.1299/jsmea.42.249.

Qiu, H. and Li, F. (2022), "Bolt looseness monitoring based on damping measurement by using a quantitative electro-mechanical impedance method", *Smart Mater. Struct.*, **31**(9), 095022. https://doi.org/10.1088/1361-665X/ac80e1.

Wan, H.P. and Ni, Y Q. (2019), "Bayesian multi-task learning methodology for reconstruction of structural health monitoring data", *Struct. Health Monit.*, **18**(4), 1282-1309. https://doi.org/10.1177/1475921718794953.

Wan, H.P. and Ni, Y.Q. (2018), "Bayesian modeling approach for forecast of structural stress response using structural health monitoring data", *J. Struct. Eng.*, **144**(9), 04018130. https://doi.org/10.1061/(ASCE)ST.1943-541X.0002085.

Wan, H.P., Zhu, Y.K., Luo, Y. and Todd, M.D. (2024), "Unsupervised deep learning approach for structural anomaly detection using probabilistic features", *Struct. Health Monit.*, https://doi.org/10.1177/14759217241226804.

Zhao, S., Fan, S., Yang, J. and Kitipornchai, S. (2023), "Numerical and experimental investigation of electro-mechanical impedance based concrete quantitative damage assessment", *Smart Mater. Struct.*, **29**(5), 055025. https://doi.org/10.1088/1361-665X/ab58e9.